Optical, Magnetic, and Electronic Properties of Peripherally Fused Macrocycles: Molybdocene Porphyrazines

Kaiming Deng, Zenong Ding, and D. E. Ellis*

Department of Physics and Astronomy and Materials Research Center, Northwestern University, Evanston, Illinois 60208

Sarah L. J. Michel and Brian M. Hoffman

Department of Chemistry and Materials Research Center, Northwestern University, Evanston, Illinois 60208

Received October 23, 2000

Metal-free and copper porphyrazines, [H_2pz] and [Cu pz], have been fused at the periphery with molybdocene dithiolene, [Cp_2Mo]. The optical, magnetic, and electronic properties of the resulting neutral and cationic complexes are studied, using first-principles density functional theory implemented by the discrete variational method. Analysis of the charge and spin distribution shows that the porphyrazine core is strongly coupled with the peripheral complex. The calculated optical absorption is found to be in reasonable agreement with experimental spectra, lending support to our theoretical model. Under appropriate circumstances one observes interaction of unpaired spins localized in the vicinity of both metal sites. The calculated spin distribution shows that [Cp_2Mo][Cu pz] and [Cp_2Mo][H_2pz]$^+$ have a magnetic moment of 1 μ_B while [Cp_2Mo][Cu pz]$^+$ and [Cp_2Mo][H_2pz] have no moment, in good agreement with the results of X-band EPR spectra. The Cu−Mo magnetic interaction is antiferromagnetic, being mediated by pyrrol nitrogens, meso nitrogens, carbons, and sulfurs.

I. Introduction

Tetraazaporphyrin (porphyrazine, pz) macrocycles have been synthesized and analyzed experimentally.[1−10] Theoretical works on pz macrocycles have been mostly concentrated on those containing a single central ion.[11−15] Our present focus is on *multimetallic* pz systems and their eventual metal−metal interactions. The considerable interest in these macrocycles is due to their high synthetic possibilities, rich coordination chemistry, and promising technological applications in catalysis,[15] in electron-transfer,[16] and as molecular electronic[17] or magnetic[18] devices, as well as their biological importance.[10] Metal ions have been fused to pz centrally and peripherally.[5,19] Because of the diffuse nature of pz's π electronic structure, it is understood that there are long-range interactions between different parts of the molecule. Thus the electronic and magnetic properties of these molecular compounds should be appreciably sensitive to the nature of substituent ions and peripheral complexes. Among several bimetallic pz synthesized, metallocene porphyrazine complexes such as ([Cp_2Mo][M(pz-((S_2);(B_2)$_3$))]),[19] in which a molybdocene moiety [Cp_2Mo] is covalently attached to a dithiolene binding site on the macrocyclic periphery, have drawn special attention due to their magnetic properties. Here M represents copper or two hydrogens at the porphyrinic center, and B is *tert* -butylphenyl or propyl attached to the macrocyclic periphery. In this paper we shall be concerned with the species 1:3 molybdocene dithiolene porphyrazine (Figure 1) with either Cu or H_2 at the center. For simplicity, we denote these as [Cp_2Mo][Cu pz] and [Cp_2Mo]-[H_2pz], respectively; for further brevity we also use the notation [Mo/Cu] and [Mo/H_2]. The cationic species [Cp_2Mo][Cu pz]$^+$

(1) Newcomb, T. P.; Godfrey, M. R.; Hoffman, B. M.; Ibers, J. A. *Inorg. Chem.* **1990**, *29*, 223−228.
(2) Natan, M. J.; Kuila, D.; Baxter, W. W.; King, B. C.; Hawkridge, F. M.; Hoffman, B. M. *J. Am. Chem. Chem.* **1990**, *112*, 4081−4082.
(3) Quirion, G.; Poirier, M.; Liou, K. K.; Hoffman, B. M. *Phys. Rev. B* **1991**, *43*, 860−864.
(4) Murata, K.; Liou, K.; Thompson, J. A.; McGhee, E. M.; Rende, D. E.; Ellis, D. E.; Musselman, R. L.; Hoffman, B. M.; Ibers, J. A. *Inorg. Chem.* **1997**, *36*, 3363−3369.
(5) Baumann, T. F.; Nasir, M. S.; Sibert, J. W.; White, A. J. P.; Olmstead, M. M.; William, D. J.; Barrett, A. G. M.; Hoffman, B. M. *J. Am. Chem. Soc.* **1996**, *118*, 10479−10486.
(6) Siber, J. W.; Baumann, T. F.; William, D. J.; White, A. J. P.; Barrett, A. G. M.; Hoffman, B. M. *J. Am. Chem. Soc.* **1996**, *118*, 10487−10493.
(7) Baumann, T. F.; Siber, J. W.; Olmstead, M. M.; Barrett, A. G. M.; Hoffman, B. M. *J. Am. Chem. Soc.* **1994**, *116*, 2639−2640.
(8) Rosa, A.; Baerends, E. J. *Inorg. Chem.* **1992**, *31*, 4717−4726.
(9) Rosa, A.; Baerends, E. J. *Inorg. Chem.* **1993**, *32*, 5637−5639.
(10) Rosa, A.; Baerends, E. J. *Inorg. Chem.* **1994**, *33*, 584−595.
(11) Liou, K.; Newcomb, T. P.; Heagy, M. D.; Thompson, W. B.; Musselman, R. L.; Jacobsen, C. S.; Hoffman, B. M.; Ibers, J. A. *Inorg. Chem.* **1992**, *31*, 4517−4523.
(12) Fourmigué, M.; Lenoir, C.; Coulon, C.; Guyon, F.; Amaudrut, J. *Inorg. Chem.* **1995**, *34*, 4979−4985.
(13) Liang, X. L.; Flores, S.; Ellis, D. E.; Hoffman, B. M.; Musselman, R. L. *J. Chem. Phys.* **1991**, *95*, 403−417.
(14) Guo, L.; Ellis, D. E.; Hoffman, B. M.; Ishikawa, Y. *Inorg. Chem.* **1996**, *35*, 5304−5312.
(15) Dailey, K. K.; Yap, G. P. A.; Rheingold, A. L.; Rauchfuss, T. B. *Angew. Chem., Int. Ed. Engl.* **1996**, *35*, 1833−1835.
(16) Schmidt, E. S.; Calderwood, T. S.; Bruice, T. C. *Inorg. Chem.* **1986**, *25*, 3718−3720.
(17) Crossley, M. J.; Burn, P. L.; Langford, S. J.; Prashar, J. K. *J. Chem. Soc., Chem. Commun.* **1995**, 1921−1923.
(18) Miller, J. S.; Vazquez, C.; Calabrese, J. C.; McLean, R. S.; Epstein, A. *J. Adv. Mater.* **1994**, *6*, 217−221.
(19) Goldberg, D. P.; Michel, S. L. J.; White, A. J. P.; Williams, D. J.; Barrett, A. G. M.; Hoffman, B. M. *Inorg. Chem.* **1998**, *37*, 2100−2101.

10.1021/ic0011664 CCC: $20.00
Published on Web 02/13/2001

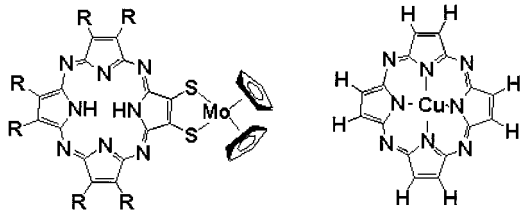

Figure 1. Schematics of molecular structures for: (a,b) [Cp_2Mo]-dithiolene-[H_2 pz], (c) isolated [Cu pz].

and [Cp_2Mo][H_2pz]$^+$ are obtained from [Mo/Cu] and [Mo/H_2] through $FcPF_6$ (Fc = ferrocenium) oxidation.

Concerning the magnetic properties of the molybdocene porphyrazines mentioned above, fluid- and frozen-solution EPR spectra[19] indicate that [Cp_2Mo][Cu pz] has a magnetic moment of 1 μ_B which was assigned to $S = {}^1/_2$ at the Cu center, corresponding to the expected Cu^{2+} d^9 configuration. The fluid-solution X-band EPR spectrum of [Cp_2Mo][H_2pz]$^+$ also exhibits a 1 μ_B magnetic moment, which was regarded as $S = {}^1/_2$ at the Mo site, corresponding to the Mo^{5+} d^1 configuration. On the other hand, the fluid- and frozen-solution EPR spectra demonstrate that [Cp_2Mo][Cu pz]$^+$ has no magnetic moment. According to interpretation of electrochemical data on the isolated compounds and the above-mentioned EPR data, it would be expected that one-electron oxidation of [Mo/Cu] occurs at the Mo position, so it was suggested[19] that there are two paramagnetic centers, at Cu^{2+}($S={}^1/_2$) and at Mo^{5+}($S={}^1/_2$), in the cation. Observation of a total magnetic moment of zero would then imply that the Cu and Mo spins are antiferromagnetically coupled to a singlet state. Considering that Cu and Mo are more than 7 Å apart in the compound, a direct antiferromagnetic coupling would be expected to be quite weak. Previous theoretical studies[13] on pz with a single metal ion have shown that the $S = {}^1/_2$ magnetization is in fact partially distributed onto the pyrrol ligands, and to a lesser extent, onto the carbon skeleton. A similar delocalization of the Mo spin onto the [Cp_2-Mo] ligands would be expected, so a second possibility exists: that of mutual spin annihilation due to delocalization. Thus the magnetic interactions within [Cp_2Mo][Cu pz]$^+$ are open to question. A theoretical study which can help to resolve this question and explore further the magnetic and electronic properties of these interesting bimetallic compounds is presented here.

Analysis of the charge and spin densities of [Cp_2Mo][Cu pz] and [Cp_2Mo][H_2pz] and their cations has been performed, using density functional theory implemented by the discrete variational method. Mulliken atomic orbital population analysis, volume-integrated density analysis, and densities of states are used to interpret the charge and spin distribution of neutral and oxidized state. Calculated optical absorption is compared with experimental spectra. In what follows, we describe our theoretical model and parameters in section II, interpret the charge and spin distributions and optical spectra in section III, discuss the magnetic interactions in section IV, and give our conclusions in section V.

II. Theoretical Model

The geometric structure of crystalline [Cp_2Mo][H_2pz] has been determined by X-ray diffraction analysis,[19] showing that there are two distinct molecules per unit cell. In one, Mo lies almost in the N_8 porphyrazine plane (displacement of 0.15 Å) and is called the "planar" geometry in the following. The second molecule is characterized by a Mo displacement of 1.17 Å above the pz plane. Density functional calculations were made on both structures, and on structures with the [Cp_2Mo] moiety folded at several different angles around the S_2 "hinge". The planar geometry for which we carry out a detailed analysis is shown schematically in Figure 1. Consistent with experimental data on many porphyrin derivatives, we will assume in the following that the geometry of the Cu-containing compound is identical to that of the measured Cu-free solid. We also suppose that the oxidized molecules [Mo/Cu]$^+$ and [Mo/H_2]$^+$ take the same structure, although this is less certain, as discussed below.

In the computations, we generally substituted the peripheral *tert*-butylphenyl terminal groups with H atoms. Selective calculations on a more complete model showed no significant changes to the results in the relevant molecular regions. It should also be pointed out that the calculations here were all made on isolated molecules, so the steric interactions of the solid, with counterions, and their effects on geometry are omitted. Use of electronic structures of free molecules in interpreting properties of weakly bonded molecular solids is a commonly used and successful strategy.[8−10,13,14]

The DF-DV scheme has been successfully used to describe physical properties such as geometric and electronic structure, and spectroscopic properties for many varied materials,[20−23] which include porphyrins and porphyrin-like molecules.[13,14] Since the DF-DV method has been described in detail elsewhere,[20,23] we will not give a further description. Suffice it to say that we used the Vosko−Wilks−Nusair spin-polarized exchange-correlation potential V_{xc} throughout the present work. The molecular Coulomb potential was generated with the help of a least-squares density-fitting scheme, using the so-called self-consistent multipolar approach. Numerical atomic basis functions used to represent the variational expansion of valence electron orbitals were 3d, 4s, 4p for Cu, 4d, 5s, 5p for Mo, 2s, 2p for C and N, and 3s, 3p for S. The inner-shell orbitals were treated as a frozen core; the valence functions were explicitly orthogonalized against the core. The Cu and Mo basis sets were generated from ionic configurations derived from the self-consistent molecular potentials (see below), while the ligand bases were taken as neutral free atom configurations. In addition to this minimal basis, we also considered an *extended basis* in which 3s, 3p C and N functions were included. As only small quantitative differences appear in occupied states, we focus in the following upon the minimal basis results.

III. Electronic Structure and Optical Spectra

Two distinct types of charge distribution analysis were made: by analytic Mulliken atomic orbital populations, and by atomic-volume integration of the self-consistent density.The two analyses give a complementary and reinforcing view of the electronic distribution; of course neither is invariant to choice of parameters: notably AO basis set, and geometric definition of atomic volumes. The volume charges presented in Table 1 were obtained by integration of the molecular density with "soft-ion" weight functions localized at the various nuclei. The weight-function radii (rollover points) were chosen as 0.5 Å for Cu, Mo, and H and 1.0 Å for the remaining atoms.

Table 1 gives a volume charge and spin analysis for the two molecules [Cp_2Mo][Cu pz] and [Cp_2Mo][H_2pz], each with two oxidation states. We have summed the individual atomic data to describe distinct, chemically related (not necessarily symmetry equivalent) sets of atomic fragments. To obtain the most compact representation, we have further summed the fragments to describe nine chemically distinct environments labeled as [Cu/

(20) Ellis, D. E.; Guenzburger, D. The Discrete Variational Method and its Applications to Large Molecules and Solid-State Systems. *Adv. Quantum Chem.* **1999**, *34*, 51−141.
(21) Deng, K.; Yang, J.; Xiao, C.; Wang, K. *Phys. Rev. B* **1996**, *54*, 2191−2197.
(22) Deng, K.; Yang, J.; Xiao, C.; Wang, K. *Phys. Rev. B* **1996**, *54*, 11907−11910.
(23) Delley, B.; Ellis, D. E. *J. Chem. Phys.* **1982**, *76*, 1949−1960.

Table 1. Volume Charge and Spin Distributions[a]

		[Cp_2Mo][Cu pz]		[Cp_2Mo][Cu pz]$^+$		[Cp_2Mo][H_2pz]		[Cp_2Mo][H_2pz]$^+$	
		charge	spin	charge	spin	charge	spin	charge	spin
Cu pz	Cu/H_2	+2.28	+0.28	+2.28	+0.33	+0.19	+0.00	+0.20	+0.00
	4N	−1.35	+0.27	−1.31	+0.22	+0.16	+0.00	+0.19	+0.02
	4N	−0.30	+0.22	−0.19	+0.04	−0.21	+0.00	−0.13	+0.03
	8C	−1.64	+0.32	−1.48	+0.08	−1.38	+0.00	−1.25	+0.01
	6C	−1.02	+0.20	−0.88	+0.03	−0.95	+0.00	−0.83	+0.00
	2C	−0.81	+0.03	−0.79	−0.02	−0.76	+0.00	−0.76	+0.05
	6H	+1.07	+0.01	+1.24	+0.00	+1.08	+0.00	+1.23	+0.00
subtotal		−1.76	+1.32	−1.13	+0.69	−1.87	+0.01	−1.35	+0.08
Cp_2Mo	2S	+0.53	+0.04	+0.60	−0.01	+0.72	+0.00	+0.77	+0.12
	Mo	+2.75	−0.28	+2.77	−0.53	+2.63	−0.01	+2.68	+0.62
	10C	−2.16	−0.08	−1.97	−0.15	−2.13	−0.00	−1.87	+0.17
	10H	+0.64	−0.00	+0.73	−0.01	+0.65	−0.00	+0.77	+0.01
subtotal		+1.76	−0.32	+2.13	−0.69	+1.87	−0.01	+2.35	+0.92
total		0	1	1	0	0	0	1	1

[a] Charge and spin distributions of atomic fragments of neutral and cationic [Cp_2Mo][M pz], M = H_2 and Cu, obtained by integrated atomic-volume analysis.

H2, 4N, 4N′, 8C, 6C′, 2C″, 6H] for the [M pz] species and 2S, Mo, 10C, 10H for the [Cp_2Mo] species. Here the integer values refer to the number of atoms in each fragment. This compact set is useful in making comparisons between the different macromolecular species.

A. Neutral Species. We first present volume charge and spin analysis of fragments in Table 1. By including the two sulfurs with the [Cp_2Mo] dithiolene species and leaving the C_2 bridging atoms with [M pz] we find that [Cp_2Mo] is a charge donor, giving 1.87e and 1.76e to [H_2pz] and [Cu pz], respectively, in the neutral-molecule state. This observation bears directly upon qualitative discussions of orbital character of the wide class of metallo-1,2-enedithiolates and their reaction products;[24,25] we may further speculate that the short C−S bond lengths are due at least in part to the strong ionic forces.

In agreement with expectations based upon the simplified [CuPc] orbital model, we find [Mo/Cu] to have net spin of 1 μ_B, while [Mo/H_2] has zero net spin; however, the internal spin distribution is not as simple as supposed in the Cu^{2+} d^9 ionic model. A spin of ∼1 μ_B is distributed mostly over Cu and its pyrrole ligands as found in previous studies on porphyrazines and other porphyrin derivatives. An unexpected feature found here is the existence of of spin of ∼0.3 μ_B localized in the Mo 4d orbital, which is compensated by diffuse spin on the pz carbon framework. This feature is predicted in both [Mo/Cu] and [Mo/H_2] and is sensitive to the ordering of several nearly degenerate orbitals close to the Fermi energy. It would be interesting to further investigate the ground state and low-lying magnetic excitations by means of total energy studies; however, that is beyond the scope of the present work.

Turning to the Mulliken analysis of the neutral [Mo/Cu] species, we find that the self-consistent configuration of $Mo^{+2.82}$ $d^{3.05}$ $s^{0.06}$ $p^{0.07}$ is notably different from the nominal ionic state Mo^{4+} d^2 s^0 p^0, due to covalent bonding interactions with Cp_2 and dithiolene ligands. The atomic configuration of $Cu^{+1.72}$ $d^{9.00}$ $s^{0.18}$ $p^{0.11}$ is also less ionic than the formal Cu^{2+} d^9 s^0 p^0 state; typical Cu charges of ∼1.5e are reported in DF-DV calculations on isolated Cu porphyrin derivatives, including [Cu pz].[14,26−28]

For the [Mo/H_2] case, we see a metal configuration $Mo^{+2.34}$ $d^{3.53}$ $s^{0.06}$ $p^{0.07}$ with ∼0.5e greater 4d occupancy than that of [Mo/Cu]. Thus we see how molybdocene reacts to the reduced electron-withdrawing power of central H_2 versus Cu in the pz macrocycle.

B. Oxidized Species. Upon oxidation, we find that the charge is redistributed on both [Cp_2Mo] and [M pz] constituents, due to the diffuse ligand valence structure. According to both volume integration and Mulliken analysis, in [Mo/Cu]$^{+1}$ ∼0.38e has been removed from [Cp_2Mo] and ∼0.62e from [Cu pz]. Thus, while the oxidation potential of isolated [Cp_2Mo] is relatively low, the attached porphyrazine unit here provides a facile electron reservoir. However, if we examine the overall volume charges, [Cp_2Mo]$^{+1.85}$[Cu pz]$^{-0.85}$, we can see that in a certain sense [Cp_2Mo] is the net electron donor. In previous electrochemical studies on dithiolene complexes, it was inferred that oxidation involves both the Mo atom and dithiolene ligand,[12] so a simple atomic Mo^{4+} → Mo^{5+} transition is not really expected. The self-consistent configuration of $Mo^{+2.81}$ $d^{3.06}$ $s^{0.07}$ $p^{0.07}$ found for [Mo/Cu]$^+$ is hardly different from that of the neutral molecule. The great stability of the "Cu d^9" configuration is also noted, with value $Cu^{+1.72}$ $d^{9.00}$ $s^{0.18}$ $p^{0.11}$ in the oxidized state pointing to the diffuse electronic orbitals of pz and the Cp_2-dithiolene units as the principal reservoirs for charge donation. This is fully consistent with previous studies on complexes like [Cu(TPP$^\bullet$)]$^+$ (TPP = tetra-*p*-tolylporphyrinate) where it was established that the first oxidation occurs from the porphyrin ring and not the copper.[29] For the [Mo/H_2]$^+$ case, we see that the self-consistent metal configuration $Mo^{+2.34}$ $d^{3.54}$ $s^{0.07}$ $p^{0.07}$ is almost identical to that of the neutral species, despite the local 4d spin moment.

According to the previous discussion we expect, and find, a net spin of zero on [Mo/Cu]$^+$ and a spin of 1 μ_B in [Mo/H_2]$^+$. In the case of [Mo/Cu]$^+$ the internal magnetization is seen to be sizable, with antiferromagnetic alignment of the Cu-centered and Mo-centered distributions. In the present model, with a thermal distribution of Fermi−Dirac occupation numbers chosen to span a dense set of nearly degenerate levels near E_F, a net volume spin of ±0.69 μ_B is found on each molecular component. For [Mo/H_2]$^+$ the net spin is rather localized on Mo as expected

(24) Fourmigue, M. *Coord. Chem. Rev.* **1998**, *178−180*, 823−864.
(25) Hsu, J. K.; Bonangelino, C. J.; Kaiwar, S. P.; Boggs, C. M.; Fettinger, J. C.; Pilato, R. S. *Inorg. Chem.* **1996**, *35*, 4743−4751.
(26) Guo, L.; Ellis, D. E.; Mundim, K. C. Hoffman, B. M. *J. Porphyrins Phthalocyanines* **1998**, *2*, 1−14.
(27) Guo, L.; Ellis, D. E.; Gubanova, O. V.; Hoffman, B. M. *Proc. Symp. Mater. Res. Soc.* **1995**, *393*, 137−142.
(28) Berkovitch-Yellin, Z.; Ellis, D. E. *J. Am. Chem. Soc.* **1981**, *103*, 6066−6073.
(29) Scholz, W. F.; Reed, C. A.; Lee, Y. J.; Scheidt, W. R.; Lang, G. *J. Am. Chem. Soc.* **1982**, *104*, 6791−6793.

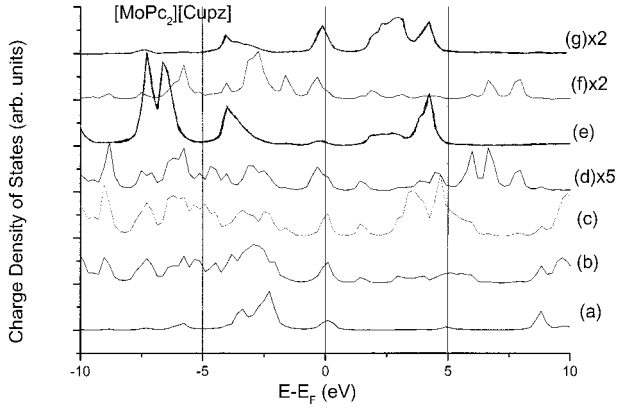

Figure 2. Partial *charge* densities of states for selected atoms of neutral [Cp_2Mo][Cu pz]: (a) Cu 3d,4sp, (b) N 2sp, (c) pz C 2sp, (d) bridge C 2sp, (e) Cp_2 C 2sp, (f) S 3sp, (g) Mo 4d,5sp. Individual curves are offset vertically for easy viewing; the notation ×2, ×5, etc. indicates multipliers used to make features more visible.

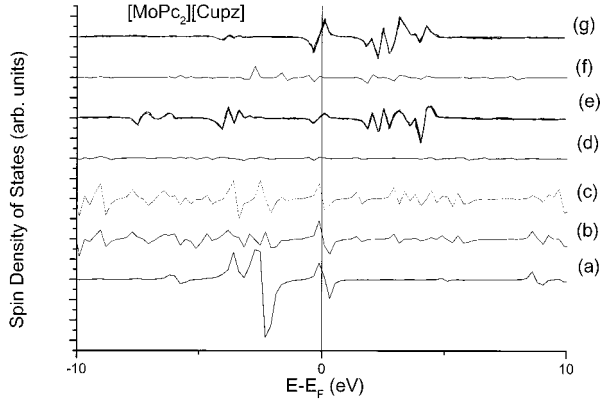

Figure 3. Partial *spin* densities of states for selected atoms of neutral [Cp_2Mo][Cu pz]: (a) Cu 3d,4sp, (b) N 2sp, (c) pz C 2sp, (d) bridge C 2sp, (e) Cp_2 C 2sp, (f) S 3sp, (g) Mo 4d,5s.

(0.62 μ_B), with delocalization of ∼0.18 μ_B onto the Cp rings and ∼−0.12 μ_B onto sulfurs. We have noted that the Mo s,p,d populations are hardly changed upon oxidation of the complex; this means simply that the metal spin polarization is achieved by the mechanism of stabilized exchange splitting, and not by charge transfer.

Considerable discussion appears in the literature on the nature of intramolecular magnetic interactions of metalloporphyrin complexes, particularly between metal-d and ring-π orbitals. In cations like $[Cu^{II}(TPP)]^+$ (TPP = tetraphenylporphyrinate),[29] $[FeCl(TPP)]^+$,[35] and $[Fe(OEP^{\bullet})(X)]^+$ [30] it is established that a relatively strong antiferromagnetic coupling exists, leading to the net spin $S = 0$ in the Cu case. The strength of the coupling has been qualitatively discussed in terms of distortions from planar symmetry and symmetry-breaking by ligand attachment. These effects are all present in the complexes treated here; a detailed accounting of the effective magnetic coupling strengths and resulting Heisenberg−Hamiltonian parameters would best be treated in terms of a *magnetic transition state* analysis.[31]

C. Partial Densities of States. Partial densities of states (PDOS) were calculated by weighting individual energy levels according to the Mulliken atomic orbital populations of the desired species. The energy levels were broadened by a Lorentzian line shape to obtain continuous curves, in the usual fashion. Analyses were made for both *charge* and *spin* distributions. PDOS for the valence orbital charge distribution of neutral [Cp_2Mo][Cu pz] are presented in Figure 2; the corresponding spin distribution is analyzed in Figure 3. Here we see the contributions of Cu and Mo, along with porphyrazine N, N′, skeleton C, C′ bridging C″, cyclopentadienyl C, and sulfur. We can interpret these results as follows:

(1) The Cu "d-band" is centered ∼3 eV below the Fermi energy E_F, with a bonding "tail" extending down to −6 eV due to covalent interaction with its N neighbors. The half-occupied topmost level (with $x^2 - y^2$ symmetry in the idealized planar D_{4h} porphyrazine) is pinned at E_F. This polarized state couples through N → C, C′(pz) → C″(bridge) to Mo to induce a polarization wave on each site, as seen in Figure 3, where the spin coupling in the HOMO at E_F is very evident.

(2) The pz N and pz C form very broad bands, consistent with the diffuse nature of the macrocycle valence states, extending to more than 15 eV above and below E_F. These states form the electron reservoir which is first affected by oxidation or reduction, and form the screening charge distribution through which the metals "see" their environment.

(3) The Cp carbon atoms form a distinct energy distribution which has little in common (although spanning a similar energy range) with the pz valence structure. Strong covalent interaction with Mo spd states is seen in the band at ∼4 eV below E_F, with similar strong antibonding features at $\sim E_F + 4$ eV.

(4) The Mo 4d, 5sp distribution shows covalent contributions ∼4 eV below E_F, as just mentioned; in addition, a sharp nearly pure 4d peak corresponding to the traditional Mo^{IV} d^2 levels is pinned at E_F.

D. Optical Absorption. Visible optical absorption spectra were obtained, as shown in Figures 4 and 5. Theoretical absorption profiles were calculated in the one-electron approximation with dipole selection rules. Excitation energies $\epsilon_f - \epsilon_i$ and oscillator strengths f_{if} were calculated using wave functions of the ground state potential. The general features are in fairly good agreement, once a blue-shift of ∼100 nm is imposed upon theoretical spectra obtained from the ground state potential. Part of this shift might be recovered by performing *transition state* calculations to include electronic relaxation in the excited state. However, we are interested here primarily in identifying significant features and their changes with composition/ionization, and previous DF−DV calculations on porphyrinic species have shown that transition state energy shifts are nearly uniform due to the diffuse nature of the important orbitals. Therefore, transition state calculations are not presented here.

It has been noted that the optical absorption bands of [M pz][Cp_2Mo] are considerably different from those of the parent compounds, and this was taken as evidence of strong coupling between the pz macrocycle and the peripheral [Cp_2Mo] moiety.[19] We therefore explored the atomic composition of initial and final state contributions to the oscillator strengths by "masking off" selected components of the LCAO-expanded molecular wave functions. We find that a large number of transitions contribute to the observed broad absorption bands, with significant components from *all* C and N framework atoms. This could have been expected from the very broad overlapping spectral distributions of the partial densities of states described

(30) Schulz, C. E.; Song, H.; Mislankar, A.; Orosz, R. D.; Reed, C. A.; Debrunner, P. G.; Scheidt, W. R. *Inorg. Chem.* **1997**, *36*, 406−412.
(31) Flores, S.; Ellis, D. E. *Inorg. Chem.* **1998**, *37*, 6346−6353, and references therein.
(32) Fourmigue, M.; Domercq, B.; Jourdain, I. V.; Molinie, P.; Guyon, F.; Amaudrut, J. *Chem.−Eur. J.* **1998**, *4*, 1714−1723.
(33) Jourdain, I. V.; Fourmigue, M.; Guyon, F.; Amaudrut, J. *J. Chem. Soc., Dalton Trans.* **1998**, 483−488.
(34) Guyon, F.; Fourmigue, M.; Audebert, P.; Amaudrut, J. *Inorg. Chim. Acta* **1995**, *239*, 117−124.
(35) Guyon, F.; Fourmigue, M.; Clerac, R.; Amaudrut, J. *J. Chem. Soc., Dalton Trans.* **1996**, 4093−4098.

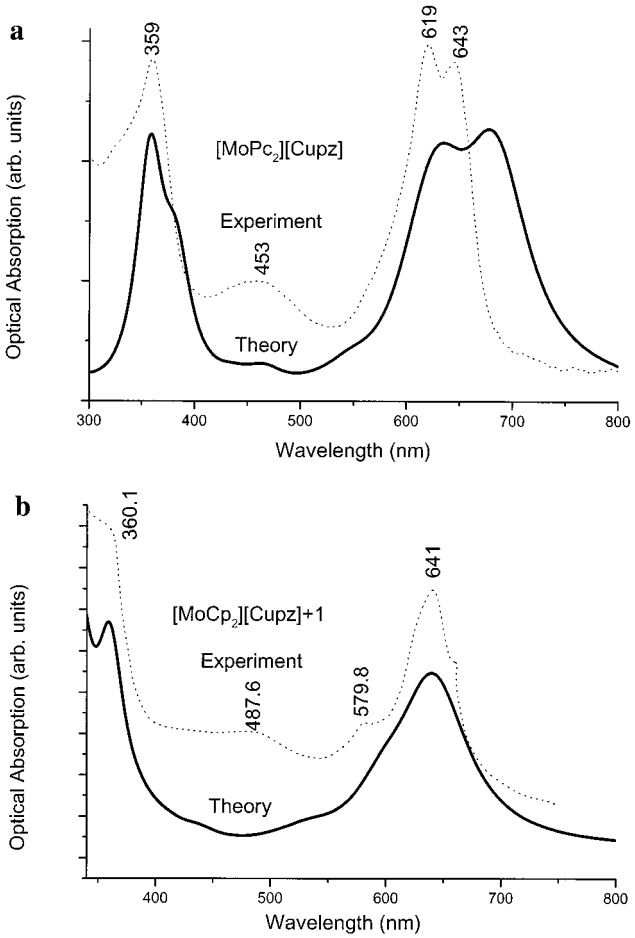

Figure 4. Optical absorption spectra for $[Cp_2Mo][Cu\ pz]$: (a) neutral species, (b) oxidized species. Calculated absorption, in dipole approximation, is given as a solid line; measured absorption as a broken line. Theoretical spectra have been shifted to align the principal CT peak with experiment (see text).

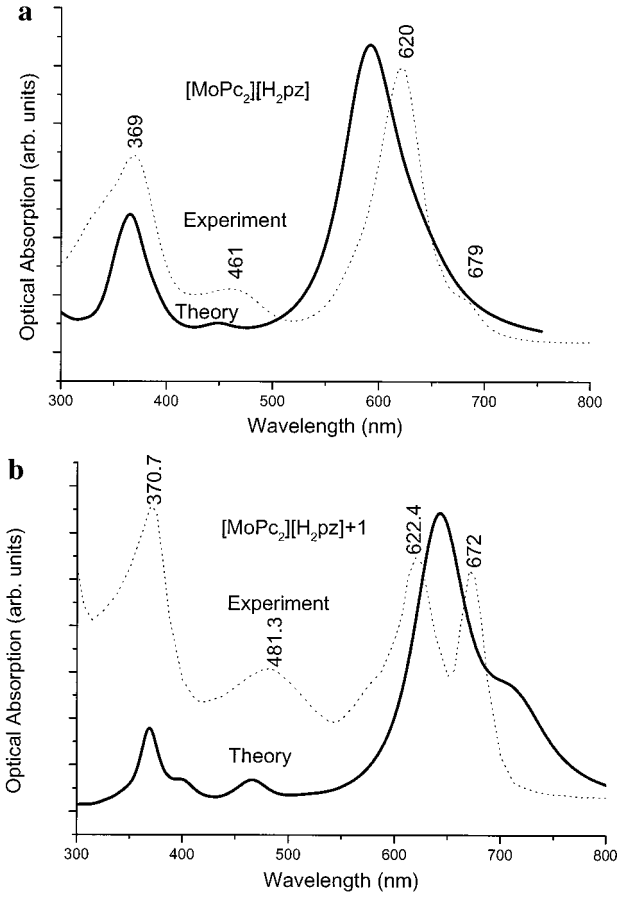

Figure 5. Optical absorption spectra for $[Cp_2Mo][H_2pz]$: (a) neutral species, (b) oxidized species. Calculated absorption, in dipole approximation, is given as a solid line; measured absorption as a broken line. Theoretical spectra have been shifted to align the principal CT peak with experiment (see text).

above. In addition to the marked metal (Cu and Mo) contributions from the critical states at $E \sim E_F$, we find that the covalency-delocalized valence- and conduction-band mixed metal/ligand character also contributes over a wide energy range.

We may characterize the experimental absorption as follows:

(1) Neutral [Mo/Cu] shows a strong visible absorption band of ∼100 nm width, with two resolved peaks at ∼643 and 619 nm. A second weaker band is centered at ∼460 nm, followed by onset of strong "charge-transfer" (CT) transitions at ∼453 nm, with a distinct peak at ∼359 nm.

(2) For the oxidized $[Mo/Cu]^+$ species, the long-wavelength (∼641 nm) peak is reduced in intensity and an additional shoulder appears in the absorption at ∼580 nm. The broad band centered at ∼488 nm appears to be slightly red-shifted compared to the neutral molecule counterpart. The charge-transfer onset (∼400 nm) is unchanged; however, the previously well-defined CT peak is no longer resolved.

(3) Neutral $[Mo/H_2]$ shows a broad (∼150 nm width) structureless absorption centered at ∼620 nm, thus corresponding to the lower energy peak of [Mo/Cu]. The broad band at ∼461 nm is unchanged, and a well-defined CT band peak (∼369 nm) is blue-shifted slightly relative to [Mo/Cu].

(4) The cation $[Mo/H_2]^+$ has two very well resolved visible bands, centered at 672 and 622 nm, a shoulder seen at ∼570 nm, the broad absorption at ∼481 nm, onset of CT at ∼400 nm, and a well-defined CT peak at ∼370 nm. The 672 nm peak appears as a new feature, and the 481 nm band is slightly red-shifted in comparison with the neutral species.

We may make several further observations about the origin of spectral features: First, the band splitting of ∼0.15 eV seen in the long-wavelength doublet of [Mo/Cu] and $[Mo/H_2]^+$ is evidently related to the existence of an unpaired spin in those two cases. Examination of spin PDOS of [Mo/Cu] shows that the exchange splitting of the (HOMO-1) level with considerable Cu 3d character is 0.4 eV; the exchange splitting of polarized levels with dominant N_8 character is about $^1/_2$ that, with magnetic splitting decreasing rapidly with distance from the metal ion. The superposition of a considerable number of transitions with magnetic splitting near E_F is sufficient to explain the observed 0.15 eV experimental peak separations. The collapse of experimental and theoretical absorption to a single peak in the nonmagnetic $[Mo/Cu]^+$ and $[Mo/H_2]$ then follows simply.

Second, we give a few details about the considerable orbital delocalization which underlies the broad absorption bands with highly mixed orbital character, using [Mo/Cu] as an example. In terms of Mulliken populations the HOMO can be described as 11% N 2p, 16% N′ 2p, 25% pz C 2p, 17% pz C′ 2p, 14% Mo 4d, and 27% distributed over other sites. The (HOMO-1) which comes closest to the $(x^2 - y^2)$ symmetry (Cu, N, N′) HOMO of the isolated [Cu pz] consists of 24% Cu, 13% N 2p, 28% Mo 4d, and 45% distributed over other sites. Thus we see that although Cu and Mo are separated by more than 7 Å, considerable degenerate orbital mixing occurs, which helps to promote the magnetic interactions described in detail below.

The absorption profiles of the last-occupied orbitals (HOMO, HOMO-1) were calculated separately to determine their influence on the complete spectra. The oscillator strengths are spread over a wide energy range of final states; however, there is a concentration of intensity in the low-energy bands, at ~735 and ~685 nm for HOMO and HOMO-1 respectively, and also in the CT region.

IV. Magnetic Structure and EPR Spectra

EPR measurements show that both $[Mo/H_2]^+$ and [Mo/Cu] have strong EPR signals associated with an unpaired spin, $S = {}^1/_2$, while $[Mo/Cu]^+$ apparently has no net spin, $S = 0$. The calculated spin distributions given in Table 1 permit a detailed interpretation of the magnetism of these complexes, in overall agreement with the EPR measurements. The qualitive argument of antiferromagnetic spin alignment between Cu and Mo[12,19] is verified here: For $[Mo/H_2]^+$, Mo carries most of the unpaired spin (0.62 μ_B), in agreement with the simple Mo^{5+} d^1 model; except that we have noted that the atomic configuration is rather far from the nominal ionic state. The remaining spin moment is spread diffusely over sulfurs (0.12 μ_B), Cp ring (0.18 μ_B) and [H_2pz] (0.08 μ_B). This spin delocalization may be correlated with the EPR isotropic coupling constants A_{iso} found for $[Cp_2MoCl_2]^+$, $[Cp_2MoO_2CPh_2]^+$, $[Cp_2MoMeC_6H_4S_2]^+$ (ref 39), and $[Cp_2Mo(TBP)pz]^+$ and $[Cp_2Mo(n\text{-}Pr)pz]^+$ (ref 19). For the chloro and oxo compounds A_{iso} of 105 and 111 MHz, respectively, can be taken to indicate a strong Mo spin localization. For $[Cp_2MoMeC_6H_4S_2]^+$ this is reduced by a factor of 2, and for the pz complexes it becomes extremely small, suggesting successive stages of delocalization. To make this idea a bit more quantitative, we also performed calculations on a model chloride complex, by simply substituting the dithiolene groups by Cl. We find the Mo d-moment to be 0.79 μ_B in this case, thus confirming the localization/A_{iso} correlation.

For neutral [Mo/Cu], the net unpaired spin has a rather complex distribution: 0.28 μ_B on Cu, 0.49 μ_B on the N_8 ring, 0.52 μ_B on the 14 C of pz, and −0.28 μ_B on Mo. The simplest interpretation of the experimental EPR, that of a localized Cu^{2+} d^9 configuration, is certainly *not* supported by the calculations, regardless of details of the diffuse spin distribution. For $[Mo/Cu]^+$ the total magnetic moment is zero, due to antiferromagnetic coupling of equal spins on $[Cp_2Mo]$ and on [Cu pz], consistent with the simple Cu d^9−Mo d^1 coupling model. However, we find that the moment on each complex is diffuse, with magnitude 0.69 μ_B; interestingly, the metal-localized moments (Cu 0.33, Mo −0.53) are *larger* than in the $S = {}^1/_2$ neutral molecule. Previous experimental work on Cp_2M-(dithiolene) and related complexes[12,25,33−36] has shown that a significant deformation can occur upon oxidation. This deformation consists of a rotation of up to ~50° about the S_2 "hinge", depending upon the metal d-electron occupancy. This behavior was explained in terms of the qualitative Hückel molecular orbital theory for d^0, d^1, and d^2 complexes.[37] For Mo^V d^2 the angle might be expected to be 0−10°, while for the oxidized Mo^{VI} d^1 the expected angle might range from 0 to 40°. We recall further that X-ray diffraction reveals that even for neutral $[Mo/H_2]$ there exist two distinct molecules in the unit cell, one of which has a diplacement of Mo out of the pz plane.

In the case of $[Mo/Cu]^+$, rotation about S_2 would move the Mo up out of the pz plane and most likely decrease the coupling between Mo d-states and the porphyrazine. On the other hand, the resulting lowering of symmetry from the perspective of the Cu-d/ring-π interaction would be expected to increase their magnetic coupling.[38,39] Therefore, we performed a series of studies in which the $[Cp_2Mo]$ unit was systematically rotated about the S_2 hinge, and the resulting charge and spin structure was monitored. As expected, the "Mo moment" became somewhat more localized with increasing angle; however, the quantitative changes did not exceed 10% of values found for the "planar" arrangement of the neutral system. The "Cu" moment was almost completely unaffected by the peripheral geometry. Thus, we suppose that the "planar" geometry contains all the main features of the metal−metal magnetic interaction, and omit further details here.

V. Conclusions

Analyses have been made of neutral and oxidized $[Cp_2Mo]$-[Cu pz] and $[Cp_2Mo][H_2pz]$ species, using first principles density functional theory. The peripherally fused molybdocene causes only a small perturbation on the porphyrazine core, with either Cu or H_2 central cations. However, considerable delocalization of wave functions over pz and Cp_2 regions takes place, leading to strong coupling of subunit electonic properties. The $[Cp_2Mo]$ unit is most strongly affected, being a net charge donor to porphyrazine of ~1.8e in the neutral species and ~1e in the oxidized state. Experimental and theoretical optical absorption spectra have been obtained and compared. The overall agreement of theory and experiment is good, once a blue-shift of ~100 nm is applied to calculated spectra. The broad absorption bands are found to result from a multitude of closely spaced transitions, with significant contributions from the entire valence structure, reflecting the strong interaction between [M pz] and $[Cp_2Mo]$ subunits.

Consistent with analyses of EPR spectra, we find that $[Mo/Cu]^0$ and $[Mo/H_2]^+$ have a net spin of 1 μ_B in their ground state, while $[Mo/Cu]^+$ and $[Mo/H_2]^0$ display zero net magnetization. Examination of details of the spin distribution show the great stability of the [Cu pz] unpaired spin, with antiferromagnetic coupling between CuN_8-localized and (Mo−Cp_2−S)-localized densities for $[Mo/Cu/]^+$. Mo in $[Cp_2Mo]$ is found to be highly polarizable; e.g., a moment is induced in the $[Mo/Cu]^0$ ground state and compensated by polarization of the diffuse pz carbon skeleton. The ionic model of Mo^{IV} $d^2 \rightarrow Mo^V$ d^1 transition in the oxidized state is found to be inaccurate; diffuse charge transfer takes place among the coupled pz and molybdocene states. The resulting Mo-d spin moment is found to be the result of stabilized exchange splitting, approximately in a $d^{3.4}$ configuration.

Acknowledgment. This work was supported by the National Science Foundation, under the MRSEC program at the Materials Research Center of Northwestern University (DMR-9632472).

IC0011664

(36) Knox, J. R.; Prout, C. K. *Acta Crystallogr.* **1969**, *B25*, 2013−2022.
(37) Lauher, J. W.; Hoffmann, R. *J. Am. Chem. Soc.* **1976**, *98*, 1729−1742.
(38) Buisson, G.; Deronzier, A.; Duee, E.; Gans, P.; Marchon, J.-C.; Regnard, J.-R. *J. Am. Chem. Soc.* **1982**, *104*, 6793−6796.
(39) Lindsell, W. E. *J. Chem. Soc., Dalton Trans.* **1975**, 2548−2552.